J|A|C|S COMMUNICATIONS

Published on Web 12/28/2009

Highly Sequence-Dependent Formation of Fluorescent Silver Nanoclusters in Hybridized DNA Duplexes for Single Nucleotide Mutation Identification

Weiwei Guo, Jipei Yuan, Qingzhe Dong, and Erkang Wang*

State Key Laboratory of Electroanalytical Chemistry, Changchun Institute of Applied Chemistry, Chinese Academy of Sciences, and Graduate School of the Chinese Academy of Sciences, Changchun 130022, Jilin, P. R. China

Received August 21, 2009; E-mail: ekwang@ciac.jl.cn

Few-atom noble-metal nanoclusters that exhibit strong, robust, and size-dependent fluorescence emission have been developed as a new class of fluorophores in the past decade.[1−4] Especially, the synthesis of fluorescent silver nanoclusters (Ag NCs) using DNA as scaffolds in aqueous solution has attracted special attention.[4−8] Typically, these Ag fluorophores are stabilized by single-stranded DNA or oligonucleotides and exhibit outstanding spectral and photophysical properties. More importantly, the generation of these novel fluorophores is highly DNA-sequence-dependent,[6−9] and the photoluminescence (PL) emission band can be tuned throughout the visible and near-IR range just by changing the sequence of the oligonucleotide.[6] These DNA-based fluorescent materials hold great promise for many research fields, such as optical sensing, single-molecular studies, nanometer-scale device science, and DNA-based nanomachines.[4,5d−f] In this study, hybridized DNA duplexes have been developed as capping scaffolds for the generation of fluorescent Ag NCs. The formation of fluorescent Ag NCs in hybridized DNA duplex scaffolds is highly sequence-dependent and can identify a typical single-nucleotide mutation, the sickle cell mutation. The identification of single-nucleotide differences using this strategy has also been extended to more general types of single-nucleotide mismatches.

The sequences of both the 24-base target segment of the normal *Homo sapiens* hemoglobin beta chain (HBB) gene (strand A, abbreviated as Str-A) and the 24-base target segment of the variation of the HBB gene responsible for the sickle cell disease (Str-B), which have only a single-nucleotide difference, are shown in Scheme 1. To form a DNA duplex with Str-A or Str-B, a probe DNA strand (Str-C, with 30 bases) was designed on the basis of the 24-base complementary sequence of Str-B with an extra six-base cytosine loop (C6 loop). The C6 loop was inserted two bases away from the mutation point (Scheme 1) in order to capture Ag(I) ions by taking advantage of the strong and specific interaction between Ag(I) ions and cytosine[4,5b,10] and then to form the fluorescent Ag NC precursor in the later stage. A series of probe DNA strands were also designed by changing the position or length of the cytosine loop compared with Str-C [P-1 to P-6; see Figure S1 in the Supporting Information (SI)]. In a typical experiment, the probe DNA strand (2 μM) was first hybridized with Str-A and Str-B at the same concentration to form two different DNA duplexes. Next, $AgNO_3$ [6:1 Ag(I)/DNA molar ratio] was added to the DNA duplex solutions. After mixture, the solutions were stirred for 15 min and then reduced with $NaBH_4$ [1:1 Ag(I)/$NaBH_4$ molar ratio] for another 7 h. The resulting solutions were studied by UV−vis absorption and PL spectroscopy.

Scheme 1. Use of Two Different DNA Duplexes with Inserted Cytosine Loops Working as Synthetic Scaffolds To Generate Fluorescent Silver Clusters for the Identification of the Sickle Cell Anemia Gene Mutation (Black Dots Represent Hydrogen Bonds Formed in Base Pairing and Black Dashed Lines the Sugar−Phosphate Backbone)

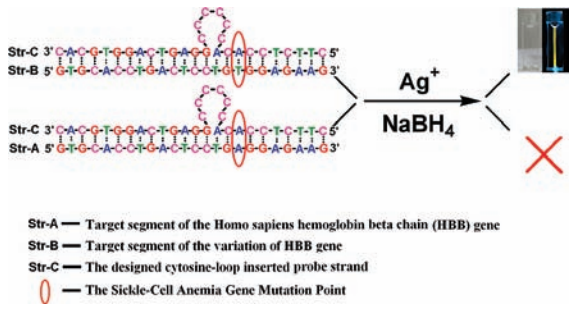

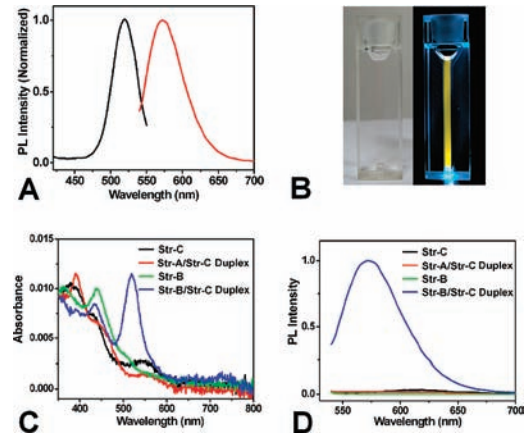

Figure 1. (A) Excitation (λ_{ex} = 520 nm) and emission (λ_{em} = 572 nm) spectra of yellow-fluorescent Ag NCs obtained using the Str-B/Str-C duplex as the synthetic scaffold. (B) Photographs of the fluorescent species generated using the Str-B/Str-C duplex as the scaffold under irradiation with (left) room light and (right) the excitation source. (C) UV−vis and (D) PL spectra under 520 nm excitation of the Ag NCs synthesized with Str-C (black line), the Str-A/Str-C duplex (red line), Str-B (green line), and the Str-B/Str-C duplex (blue line) as the scaffold. The value of 1 in (D) was set to the PL signal intensity of the Ag NCs obtained using the Str-B/Str-C duplex as the scaffold. The corresponding UV−vis spectra with a broader wavelength range are shown separately in Figure S2.

Figure 1A,B shows PL spectra and photographs of a strongly yellow-emitting silver species generated using the Str-B/Str-C duplex as the capping scaffold; the excitation and emission maxima are at 520 and 572 nm, respectively. A characteristic absorption peak with maximum wavelength and bandwidth identical to the PL excitation peak appeared in the recorded UV−vis spectrum (Figure 1C, blue line). Control experiments demonstrated that this unique PL-emitting species was not generated when either the Str-A/Str-C duplex or Str-B or Str-C single strands were used as the scaffold (red, green, and black lines, respectively, in Figure 1C,D), which confirmed that only Str-B/Str-C duplex worked as an efficient capping scaffold for this unique fluorescent silver species. The above experiments imply that the formation of Ag NCs in these DNA

10.1021/ja907075s

duplexes (Str-A/Str-C and Str-B/Str-C) is highly sequence-dependent and can identify this single-nucleotide difference. Further studies under same conditions as used with Str-B/Str-C were performed on a series of probe DNA strands formed by changing the position of the C6 loop from one to four bases away from the mutation point (Figure S1). The results showed that the distance between the position of the C6 loop and the mutation point plays an important role in the Ag NC formation. When the C6 loop was one or two bases away from the mutation point, silver species with strong PL were generated from the Str-A/P-1 and Str-B/Str-C duplexes, and identification of this mutation could be achieved (Figures S3 and S4). In comparison, only a weakly PL-emitting species was generated when the C6 loop was three bases away from the mutation point, but in this case, the identification of this single-nucleotide difference could still be achieved (Figure S5). However, when the position of the C6 loop was far from the mutation point (i.e., for P-4, in which the C6 loop is four bases away from the mutation point), the PL emission of the generated silver clusters was rather weak, and the influence of this mutation on the Ag NC formation became negligible (Figure S6). The above results indicate that when the distance between the mutation point and the C6-loop is less than three bases, strongly PL-emitting species can be generated and can distinguish the target Str-A from Str-B by comparative PL analysis of the formed silver species. Further experiments concerning the influence of size of the cytosine loop on the formation of silver clusters were carried out, and two additional probes with C4 and C8 loops two bases away from the mutation point also showed good ability to identify the two target strands (Figures S7 and S8). Among all these tested probe strands, P-1 and Str-C seemed to be the most efficient probe strands for the identification of the target Str-A and Str-B, respectively. To validate these probe strands in a practical genetic assay, a 100 base pair gene segment including the target sequence that was obtained through PCR amplification of the gene sample of a healthy individual was used as the target to carry out the Ag NC formation experiments (for details, see pp S1−S2 and Figure S9 in the SI). With the synthetic targets Str-A and Str-B as controls, the PL analysis of this real sample was in good accordance with Str-A but rather different from Str-B (Figure S10). Therefore, the obtained target segment of the HBB gene derived from the real human gene was confirmed as the normal HBB gene by this method.

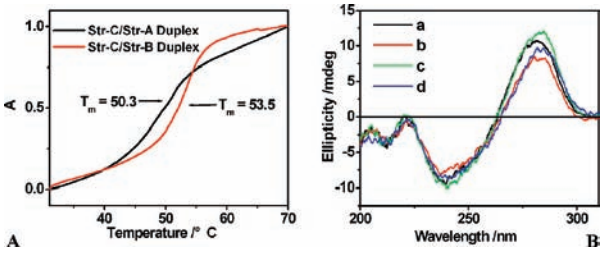

Figure 2. (A) Relative absorbance $A = [(A_t - A_{31°C})/(A_{70°C} - A_{31°C})]$ at 260 nm vs temperature (t) for Str-A/Str-C (black line) and Str-B/Str-C (red line) duplexes [2 μM in 20 mM phosphate buffer (pH 7.0) containing 1 mM magnesium acetate]. (B) CD spectra of Str-A/Str-C duplex (a, black line), a silver sample with the Str-A/Str-C duplex as the synthetic scaffold (b, red line), the Str-B/Str-C duplex (c, green line), and a silver sample with the Str-B/Str-C duplex as the synthetic scaffold (d, blue line).

In the case of forming Str-A/Str-C and Str-B/Str-C duplexes, Str-A has a single nucleotide difference compared with Str-B and can form an A:A mismatch when it hybridizes with Str-C (Scheme 1). Thermally induced transition profiles of Str-A/Str-C and Str-B/Str-C duplexes showed that the Str-B/Str-C duplex had a higher melting temperature (53.5 °C) and steeper melting transition than the Str-A/Str-C duplex (50.3 °C) (Figure 2A). These results reveal that the Str-B/Str-C duplex forms a more double-helical region than the Str-A/Str-C duplex, and the single-nucleotide mismatch obviously influences the structure of the formed duplexes. Furthermore, in comparison with the strong influence of Ag NC formation on the structure of the single-stranded DNA scaffold,[5a,b] circular dichroism (CD) spectra of Ag NCs stabilized by the Str-A/Str-C and Str-B/Str-C duplexes and related DNA duplexes suggested that these double-stranded DNA mainly keep the structure characteristic of a B-form helix (Figure 2B),[11] and the formation of Ag NCs only weakly changes the structure of the Str-A/Str-C and Str-B/Str-C duplex scaffolds under the present experimental conditions. Combined, these results imply that the single-base mismatch can influence the configuration and local nucleotide sequence of the formed cytosine loop and further can influence the formation of highly sequence-dependent fluorescent silver species[6−9] when the mutation point is adjacent to the cytosine loop.

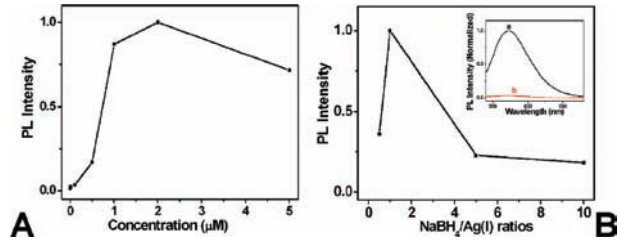

Figure 3. (A) Influence of Str-B concentration on the generation of the yellow-emitting silver species. [The PL intensity at 572 nm with $\lambda_{ex} = 520$ nm was recorded. Str-C concentration, 2 μM; Ag(I)/Str-C = 6:1; $NaBH_4$/Ag(I) = 1:1.] (B) Influence of the $NaBH_4$/Ag(I) ratio on the generation of the fluorescent silver species. Inset: PL spectra of the generated fluorescent species (a) before and (b) after reduction treatment using $NaBH_4$. [Str-C concentration, 2 μM; Ag(I)/Str-C = 6:1; the highest PL intensity was set to a value of 1.]

In the case of generation of yellow-emitting silver species with the Str-B/Str-C duplex as the scaffold, the influences of the Str-B concentration and the $NaBH_4$/Ag(I) ratio were further investigated (Figure 3). Silver species with the strongest PL emission were generated when the concentration of Str-B was the same as that of Str-C (2 μM), implying that the highly efficient formation of the Str-B/Str-C duplex is crucial to the generation of this fluorescent species (Figure 3A). The influence of the $NaBH_4$/Ag(I) ratio (Figure 3B) indicated that a high $NaBH_4$/Ag(I) ratio leads to the low-yield generation of this yellow-fluorescent silver species. Furthermore, the PL emission of Ag NCs generated with 2 nmol DNA duplex (a in the Figure 3B inset) can be fully quenched after the addition of 18 nmol of $NaBH_4$ for 15 min (b in the Figure 3B inset). These results imply that the silver species stabilized by the Str-B/Str-C duplex is probably a partly reduced Ag NC.[5b] On the basis of mass spectroscopic characterization, some studies have indicated that most reported DNA-stabilized fluorescent Ag NCs contain less than six silver atoms.[5b,6,7] However, the characterization of these duplex-capped Ag NCs by mass spectrometry was rather difficult because of the incompatibility of mass spectroscopy and buffered conditions as well as the comparatively brittle DNA duplex structure. The room-temperature PL quantum yield (QY) and excited-state lifetime of the obtained yellow-emitting silver species were estimated to be 34 ± 2% (compared with rhodamine 6G in ethanol, which has a standard QY of 95%)[12] and 2.60 ± 0.05 ns, respectively.

To extend this study from the identification of the sickle cell mutation to more general single-nucleotide mismatches, a new duplex comprising a probe strand (Str-D) and a target strand (Str-E) was designed (Figure 4A). Target strand Str-E with 30 bases

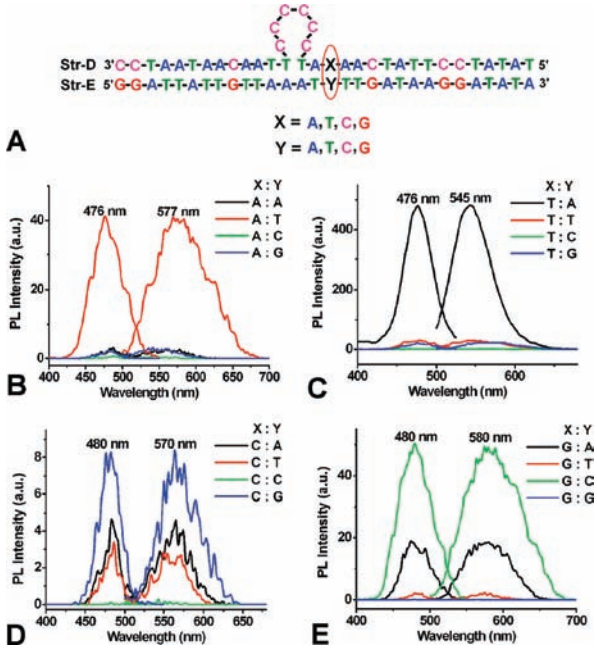

Figure 4. (A) Designed Str-D/Str-E DNA duplex with a mutation point (X:Y) two bases away from the inserted C6 loop. (B−E) PL spectra of Ag NCs obtained using the Str-D/Str-E duplex as the scaffold with Y = A, T, C, G and X = (B) A, (C) T, (D) C, and (E) G. [20 mM phosphate, 1 mM magnesium acetate (pH 7.0); Str-D/Str-E concentration, 2 μM; Ag(I)/duplex = 6:1; $NaBH_4$/Ag(I) = 1:1; reaction time, 7 h.]

was designed on the basis of the anthrax lethal factor sequence, in which the "Y"-point base is adenine. The Str-D/Str-E duplex has a mutation point (X:Y) two bases away from the inserted C6 loop. For duplex Str-D/Str-E, the bases at the "X" and "Y" points can be adenine (A), thymine (T), cytosine (C), or guanine (G). By variation of the bases at the X and Y points in Str-D and Str-E, respectively, 16 DNA duplexes that cover all kinds of single-nucleotide mismatches at the mutation point were obtained. These newly formed DNA duplexes were used as scaffolds to generate Ag NCs under the same conditions as used for the Str-A/Str-C and Str-B/Str-C duplexes, and the corresponding PL spectra are shown in Figure 4B−E. When the base at the X point of Str-D is complementary to the one at the Y point of Str-E [A:T, red line in (B); T:A, black line in (C); C:G, blue line in (D); G:C, green line in (E)], the corresponding DNA duplex-stabilized Ag NCs exhibit the highest PL emission relative to those for the other three DNA duplexes with the single-nucleotide mismatch at the X:Y point. These results demonstrate the feasibility of identifying different types of single-nucleotide mutations using the highly sequence-dependent fluorescent Ag NC formation in DNA scaffolds. It should be noted that the background DNA duplex region adjacent to the cytosine loop also has impact on the Ag NC formation. Among the four DNA duplex scaffolds with completely complementary background DNA duplex regions shown in Figure 4 [A:T, red line in (B); T:A, black line in (C); C:G, blue line in (D); G:C, green line in (E)], the generated PL from the Ag NCs differed in both PL intensity and PL bands. These differences are due to the influence of the background DNA sequence on the configuration and local nucleotide sequence of formed the cytosine loops and further on the formation of the fluorescent silver species. Thus, a systematic selection process (by varying the sequence of the probe strand) is necessary to obtain an effective probe strand that can identify two target strands with a single-nucleotide difference through the formation of fluorescent Ag NCs.

In summary, probe DNA strands designed with an inserted cytosine loop were hybridized with target strands to form duplex DNA scaffolds for the generation of fluorescent Ag NCs. The formation of fluorescent Ag NCs in these duplex scaffolds was highly sequence-dependent and able to specifically identify a typical single-nucleotide mutation, the sickle cell anemia mutation. The identification based on this strategy was further extended to more general types of single-nucleotide mismatches. This work expands the available capping DNA scaffolds of fluorescent Ag NCs from single-stranded oligonucleotides to hybridized DNA duplexes, and the highly sequence-dependent formation is likely to find use in bioanalysis fields such as DNA-hybridization-based analysis.

Acknowledgment. This research was supported by the National Natural Science Foundation of China through Grants 20675078 and 20890020 and 973 Projects 2009CB930100 and 2010CB933600.

Supporting Information Available: Experimental details; PL, UV−vis, PL delay, and CD instruments; sequences of probe strands P-1 through P-6; extended spectra of Figure 1C; PL spectra of Ag NCs generated using other probe strands (P-1 through P-6); introduction to sickle cell anemia and sickle cell disease traits; and results of the practical analysis of a human gene sample. This material is available free of charge via the Internet at http://pubs.acs.org.

References

(1) (a) Zheng, J.; Nicovich, P. R.; Dickson, R. M. *Annu. Rev. Phys. Chem.* **2007**, *58*, 409. (b) Huang, T.; Murray, R. W. *J. Phys. Chem. B* **2001**, *105*, 12498. (c) Zheng, J.; Zhang, C. W.; Dickson, R. M. *Phys. Rev. Lett.* **2004**, *93*, 077402.
(2) (a) Peyser, L. A.; Vinson, A. E.; Bartko, A. P.; Dickson, R. M. *Science* **2001**, *291*, 103. (b) Zheng, J.; Dickson, R. M. *J. Am. Chem. Soc.* **2002**, *124*, 13982. (c) Yu, J.; Patel, S. A.; Dickson, R. M. *Angew. Chem., Int. Ed.* **2007**, *46*, 2028.
(3) (a) Lesniak, W.; Bielinska, A. U.; Sun, K.; Janczak, K. W.; Shi, X.; Baker, J. R., Jr.; Balogh, L. P. *Nano Lett.* **2005**, *5*, 2123. (b) Zhang, J.; Xu, S.; Kumacheva, E. *Adv. Mater.* **2005**, *17*, 2336. (c) Shen, Z.; Duan, H.; Frey, H. *Adv. Mater.* **2007**, *19*, 349. (d) Shang, L.; Dong, S. J. *Chem. Commun.* **2008**, 1088. (e) Díez, I.; Pusa, M.; Kulmala, S.; Jiang, H.; Walther, A.; Goldmann, A. S.; Müller, A. H. E.; Ikkala, O.; Ras, R. H. A. *Angew. Chem., Int. Ed.* **2009**, *48*, 2122. (f) Maretti, L.; Billone, P. S.; Liu, Y.; Scaiano, J. C. *J. Am. Chem. Soc.* **2009**, *131*, 13972.
(4) Vosch, T.; Antoku, Y.; Hsiang, J. C.; Richards, C. I.; Gonzalez, J. I.; Dickson, R. M. *Proc. Natl. Acad. Sci. U.S.A.* **2007**, *104*, 12616.
(5) (a) Petty, J. T.; Zheng, J.; Hud, N. V.; Dickson, R. M. *J. Am. Chem. Soc.* **2004**, *126*, 5207. (b) Antoku, Y. Ph.D. Thesis, Georgia Institute of Technology, 2007. (c) Ritchie, C. M.; Johnsen, K. R.; Kiser, J. R.; Antoku, Y.; Dickson, R. M.; Petty, J. T. *J. Phys. Chem. C* **2007**, *111*, 175. (d) Yu, J. H.; Choi, S.; Dickson, R. M. *Angew. Chem., Int. Ed.* **2009**, *48*, 318. (e) Richards, C. I.; Hsiang, J. C.; Senapati, D.; Patel, S.; Yu, J. H.; Vosch, T.; Dickson, R. M. *J. Am. Chem. Soc.* **2009**, *131*, 4619. (f) Guo, W. W.; Yuan, J. P.; Wang, E. K. *Chem. Commun.* **2009**, 3395.
(6) Richards, C. I.; Choi, S.; Hsiang, J. C.; Antoku, Y.; Vosch, T.; Bongiorno, A.; Tzeng, Y. L.; Dickson, R. M. *J. Am. Chem. Soc.* **2008**, *130*, 5038.
(7) Gwinn, E. G.; O'Neill, P.; Guerrero, A. J.; Bouwmeester, D.; Fygenson, D. K. *Adv. Mater.* **2008**, *20*, 279.
(8) Sengupta, B.; Ritchie, C. M.; Buckman, J. G.; Johnsen, K. R.; Goodwin, P. M.; Petty, J. T. *J. Phys. Chem. C* **2008**, *112*, 18776.
(9) O'Neill, P. R.; Velazquez, L. R.; Dunn, D. G.; Gwinn, E. G.; Fygenson, D. K. *J. Phys. Chem. C* **2009**, *113*, 4229.
(10) Ono, A.; Cao, S.; Togashi, H.; Tashiro, M.; Fujimoto, T.; Machinami, T.; Oda, S.; Miyake, Y.; Okamoto, I.; Tanaka, Y. *Chem. Commun.* **2008**, 4825.
(11) (a) Baker, E. S.; Bowers, M. T. *J. Am. Soc. Mass Spectrom.* **2007**, *18*, 1188. (b) Poehl, F. M.; Jovin, T. M. *J. Mol. Biol.* **1972**, *67*, 375. (c) Trantirek, L.; Stefl, R.; Vorlickova, M.; Koca, J.; Sklenar, V.; Kypr, J. *J. Mol. Biol.* **2000**, *297*, 907.
(12) Kubin, R. F.; Fletcher, A. N. *J. Lumin.* **1982**, *27*, 455.

JA907075S